7-1-1999

A study of omega bands and Ps6 pulsations on the ground, at low altitude and at geostationary orbit

A. M. Jorgensen

Harlan E. Spence
Boston University, harlan.spence@unh.edu

T. J. Hughes

D. McDiarmid

A study of omega bands and Ps6 pulsations on the ground, at low altitude and at geostationary orbit

A. M. Jorgensen[1] and H. E. Spence
Center for Space Physics, Boston University, Boston, Massachusetts

T. J. Hughes and D. McDiarmid
Herzberg Institute of Astrophysics, National Research Council, Ottawa, Ontario, Canada

Abstract. We investigate the electrodynamic coupling between auroral omega bands and the inner magnetosphere. The goal of this study is to determine the features to which omega bands map in the magnetosphere. To establish the auroral-magnetosphere connection, we appeal to the case study analysis of the data rich event of September 26, 1989. At 6 magnetic local time (MLT), two trains of Ps6 pulsations (ground magnetic signatures of omega bands) were observed to drift over the Canadian Auroral Network For the OPEN Program Unified Study (CANOPUS) chain. At the same time periodic ionospheric flow patterns moved through the collocated Bistatic Auroral Radar System (BARS) field of view. Similar coincident magnetic variations were observed by GOES 6, GOES 7 and SCATHA, all of which had magnetic foot points near the CANOPUS/BARS stations. SCATHA, which was located at 6 MLT, $0.5\,R_E$ earthward of GOES 7 observed the 10 min period pulsations, whereas GOES 7 did not. In addition, DMSP F6 and F8 were over-flying the region and observed characteristic precipitation and flow signatures. From this fortunate constellation of ground and space observations, we conclude that auroral omega bands are the electrodynamic signature of a corrugated current sheet (or some similar spatially localized magnetic structure) in the near-Earth geostationary magnetosphere.

1. Introduction

Omega bands are auroral luminosity and current structures which characteristically appear as rows of inverted (if "up" is north) Ω-shaped dark patches extending south into the diffuse aurora. Omega bands generally appear during substorm recovery phase in the morning sector auroral zone. They range in sizes from hundreds to a thousand kilometers and drift eastward with a velocity of about 1 km/s, producing an associated period of about 10-20 minutes. Ps6 pulsations are 10-20 min. quasi-periodic signatures in the east-west ground magnetic field, that appear during substorm recovery phase on the morning side. It is now well known that auroral omega bands and Ps6 pulsations are the manifestation of the same phenomenon. The bright Ω band auroral patches are caused by electron precipitation, and the set of Ps6 pulsations are generated by the associated current system.

The correspondence between auroral features measured from the ground (including omega bands), and their signatures measured in the magnetosphere has been an area which has received a lot of attention over the past 25 years. *Akasofu et al.* [1971] originally suggested that auroral Ω bands (and surges), which he measured at the poleward edge of the auroral bulge, could be ripples on the surface of the plasma sheet which map to the auroral zone. This initial supposition was followed by other studies that sought empirical relationships or theoretical justification for the genesis of omega bands.
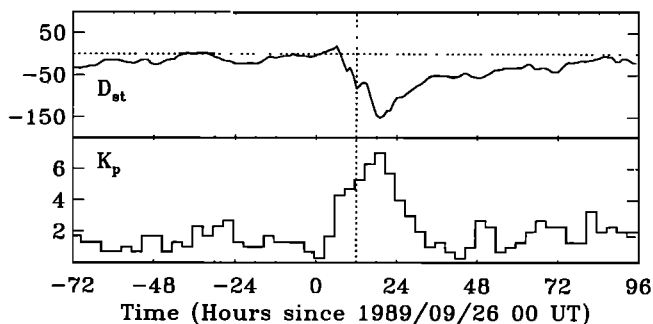
Kawasaki and Rostoker [1979] proposed an ionospheric current system responsible for Ps6 pulsations. Their model for a spatially varying current had essentially two options: a region of enhanced electric field drifting eastward, or a region of high electron precipitation drifting eastward. They proposed the later mechanism, since that could link Ps6 pulsations with the luminosity variation of auroral omega bands which have similar drift velocity and occurrence frequencies. *Rostoker and Barichello* [1980] surveyed the diurnal and seasonal occurrence rate of Ps6 pulsations. They found that the occurrence rate of Ps6 varied in such a way as to be most common between 4 and 6 local time (LT),

and approximately twice as frequent in April through August as in October through February. They noted that April through August are the months where the ambient southeastward electric field is strongest in the morning side. Thus this asymmetry supports the theory that the current structures are produced by high-conductivity regions drifting into the ambient electric field on the dawn side, rather than patches of enhanced electric field. Based on their physical model one would expect this result to apply to the northern hemisphere, and the inverse relation to the southern hemisphere (twice as frequent in October through February as April through August). As far as we know, this has not yet been tested experimentally.
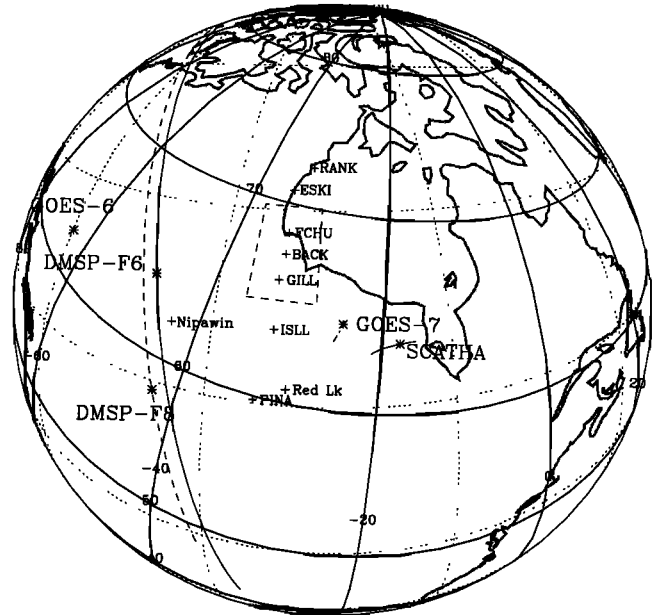
Attempts to relate omega bands to magnetospheric phenomea are exemplified in the work of *Rostoker and Samson* [1984]. They presented a substorm model which attributed Ps6 pulsations/Ω bands to a Kelvin-Helmholtz instability (KHI) between the tailward flow in the low-latitude boundary layer (LLBL) and the earthward flow in the central plasma sheet (CPS) on the dawn side. In their model the westward traveling surge was attributed to the evening side LLBL/CPS interface, and the asymmetry between them was attributed to the corotation that is dominant in the inner magnetosphere.

As empirical magnetic field models improved, direct mapping of auroral structures to the magnetosphere were attempted. *Pulkkinen et al.* [1991] used the *Tsyganenko* [1989] (T89) empirical magnetic field model to map auroral omega bands and Ps6 events to the equatorial plane. They found that the features map to between 6 and of 13 R_E between 2 and 7 MLT. These mappings did not include any field-aligned currents that are known to be strong in these regions nor was there any coincident magnetospheric observations to constrain or test the mappings.

Nevertheless, these mappings indicated a near-Earth source of omega bands within the magnetosphere. With the realization that the omega band aurora could not possibly map to the LLBL, *Connors and Rostoker* [1993] concluded that omega bands are generated at

Figure 2. This projection shows the positions of the ground data sources as well as the magnetic ground tracks of the satellites according to T89 as viewed from an altitude of 1000 km over Canada. The map shows the CANOPUS/MARIA stations, the BARS radar field of view, GOES 6 and 7, DMSP F6 (solid track) and F8 (dashed track), and SCATHA. The satellite positions at 1230 UT are marked by an asterisk. The ground stations are marked with + signs. For all but the DMSP satellites, the ground tracks are shown from 1100 to 1300 UT.

Figure 1. 7 days of Dst and K_P centered on 1200 UT on September 26, 1989. This Ps6/omega band event occurred during the main phase of a magnetic storm, at a time when Dst showed a weak recovery.

the inner edge of the plasma sheet. They maintained that the KHI was still a plausible explanation for their generation mechanism.

Common to all these papers is the limitation that all omega band/Ps6 features have been observed only on the ground (or by spacecraft auroral imagers which is qualitatively the same thing). At most, a magnetospheric source location has been inferred through simple magnetic mappings. In this paper we present an event in which the Ps6 pulsations are observed both on the ground and in the equatorial plane of the magnetosphere, inside of geostationary orbit. We find that the current systems connecting the auroral ionosphere with the magnetosphere close inside of geostationary orbit. It is interesting to note that over the last 20 years the presumed location of the magnetospheric source of Ω bands has undergone a similar earthward motion as the presumed location of substorm onsets.

2. Data Set/Observations

For this study, we focus on an event that occurred on September 26, 1989. At the time, K_P was 5, and the magnetosphere was in the main phase of a magnetic storm, Dst was -75 nT, and the storm reached a minimum of -150 nT. The Ps6 event occurred around 1200

Table 1. Positions of the Relevant CANOPUS Stations

| Station	MAG, deg		Geodetic, deg	
	Latitude	Longitude	Latitude	Longitude
Gillam	66.00	327.06	56.38	265.36
Island Lake	63.52	328.09	53.86	265.34
Pinawa	59.77	327.58	50.20	263.96

UT on this day, as indicated by the vertical dotted line in Figure 1, during a short, partial Dst recovery, and during the recovery phase of a multiple onset substorm.

Figure 2 gives a synoptic view of all the data sources used for this event. We used magnetic field data from GOES 6 and 7 and SCATHA; auroral precipitation of electrons and protons, as well as east-west flows from DMSP F6 and F8; ionospheric flows/electric fields from the CANOPUS/BARS radar array; and ground magnetometer and riometer data from the CANOPUS Magnetometer and Riometer Array (MARIA). Magnetic foot points of the geostationary spacecraft and ground tracks of the low-altitude satellites are plotted along with the CANOPUS station locations on the globe. Details of these data sets follow below. All-sky image data from the CANOPUS chain ideally could have provided a direct link between Ps6 waves and omega bands; however, these images provided no useful information as this event occurred in sunlit conditions. In the following sections all times are universal time (UT) unless otherwise specified, and all coordinates are in dipole coordinates (MAG), as defined in the GEOPACK software package by *Peredo et al.* [1995] unless otherwise specified. Table 1 lists the positions of the CANOPUS/MARIA stations used.

Figure 3 shows three-component magnetometer as well as riometer data for three CANOPUS stations at the southern end of the north-south chain. Gillam (magnetic latitude of 66°) sees strong Ps6 magnetic pulsations between 1135 and 1205 UT, exhibiting three periods of 800 nT peak-to-peak amplitude with approximately 10-min period. Positive peaks in the Y component occur at 1135, 1145, 1155 and 1205 UT. The positive peaks in X and Z components are phase delayed with respect to Y by a quarter period, characteristic of Ps6 current system. The Gillam riometer sees periodic absorptions corresponding to the positive peaks in the Y component, indicating that the peak current is also the location of the precipitation, as expected [*Kawasaki and Rostoker* [1979]]. Two additional weaker peaks can be seen in the magnetometer and riometer data at 1220-1225, and at 1235 UT.

At Pinawa station (6.2° to the south of Gillam station), three wave periods were observed between 1215 and 1250. The positive peaks in the Y component occurred at 1220, 1235 and 1247 UT. The Pinawa riometer observed the same three peaks. Note that the Pinawa signatures contain only positive field deflections in the

Y and Z components, whereas Gillam sees bipolar pulsations. At Pinawa the wave period seems to be decreasing with time. We note that, despite many data dropouts, the centrally located Island Lake station sees
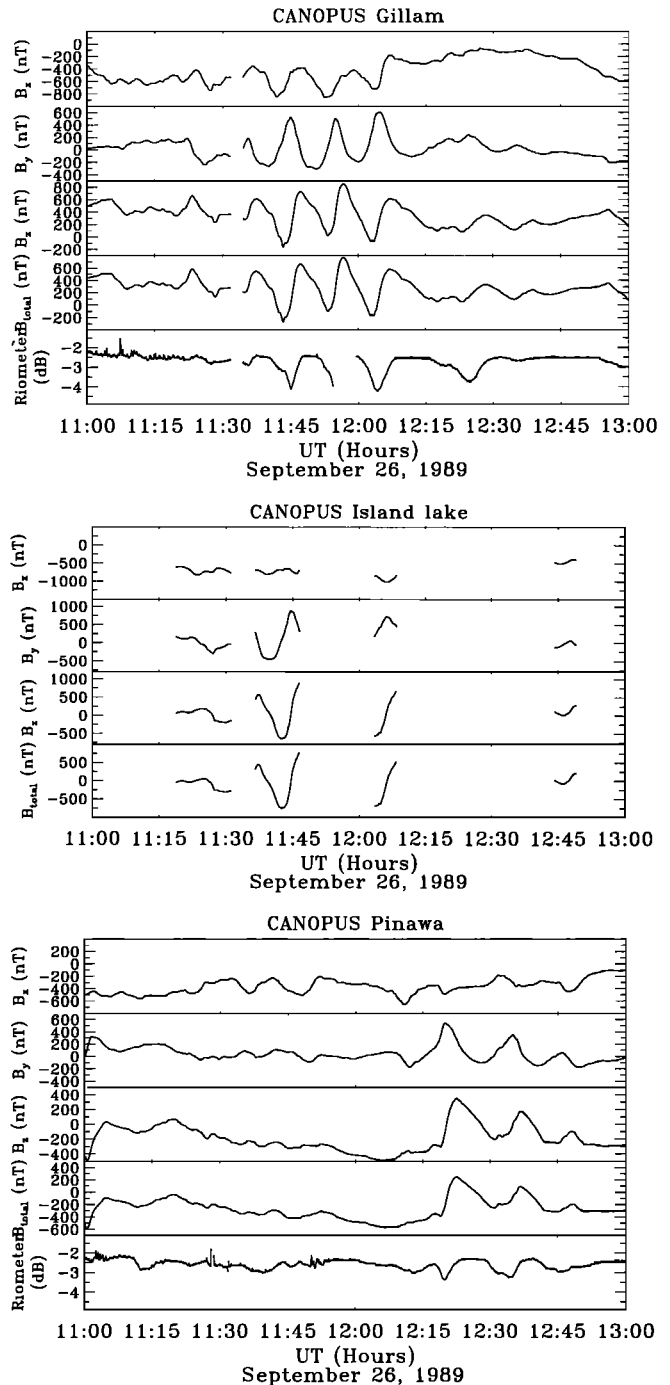
Figure 3. Magnetometer and riometer data for the three southern CANOPUS stations: Gillam, Island Lake, and Pinawa. Only these stations observed the Ps6 pulsations. A train of pulsations was first observed at Gillam, and then another train was observed at Pinawa. Both trains were observed at Island Lake which is located in between the two. Notice how the riometer absorptions are exactly aligned with the eastward perturbations.
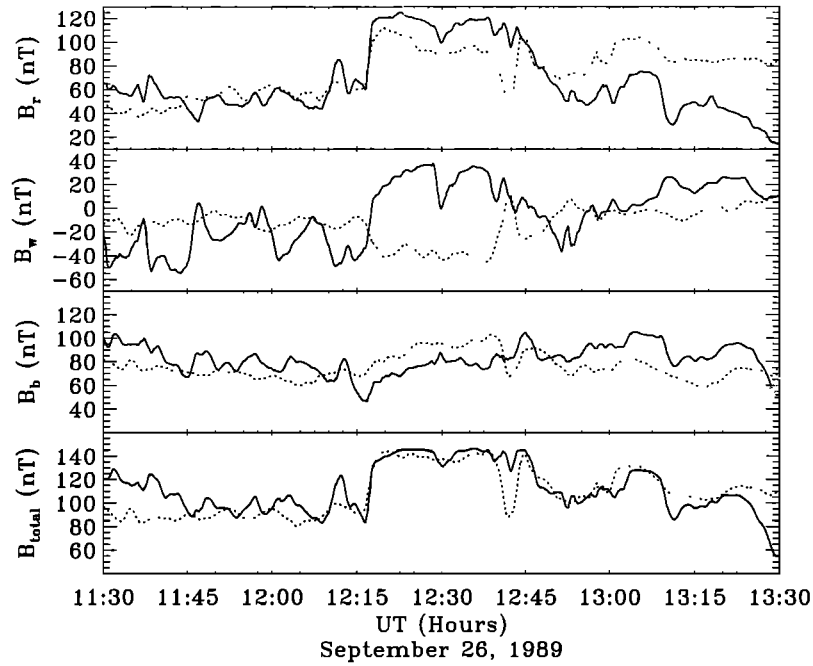
Figure 4. GOES 6 (dotted line) and 7 (solid line) see similar features but displaced in time by approximately 6.7 min. The observed signature is a stretching and rotation of the field corresponding to the eastward propagation of a earthward flowing current. Data was smoothed using a 1 min running average.

very strong signatures of both sets of magnetic pulsations, with a peak to peak amplitude greater than 1500 nT.

Figure 4 shows the GOES 6 and 7 magnetometer data. The data are given in the $\hat{r}$, $\hat{w}$, $\hat{b}$ coordinate system, which is defined based on a magnetic field model (the model by Tsyganenko [1987] (T87) in this case). The $\hat{b}$ axis is parallel to the model field. The $\hat{r}$ axis points in the direction of the locally determined radius of curvature (towards the center of curvature), and the $\hat{w}$ axis completes the right-hand coordinate system (w for "west"). Table 2 lists the positions of the three high altitude satellites at 1200 UT and at 1300 UT. Both geostationary satellites see a compressional signature of about 40 nT, and both see a strong increase in the radial component during the compression, suggesting a much more tail-like geometry than the model is able to

produce. GOES 7 sees this compression at 1215, the same time that the pulsations start at Pinawa. GOES 6 sees the same signature 6.7 min earlier, corresponding to a propagation velocity of 85 km/s along geostationary orbit from 3 MLT (GOES 6) to 6 MLT (GOES 7), or 8 km/s on the ground. GOES 6 and 7 see opposite signatures in B_w, consistent with a sheet of earthward flowing field-aligned current (FAC) located between the two spacecrafts. GOES 7 also sees weak signatures correlated with the Gillam pulsations. Note also the dip in B_r and B_w at GOES 7 at 1230 UT.

The magnitude of the magnetic field seen at SCATHA is more or less constant throughout the same time period (see Figure 5). However, the individual components vary in such a way that field line rotations occur between dipole-like (when B_r is small) and tail-like

**Table 2.** Mapped and Actual Positions of the Magnetospheric Spacecrafts

| Satellite | Time, UT | Mapped Position | | | | Position | | |
| | | Geodetic, deg | | MAG, deg | | Radius | MAG | MLT |
		Latitude	Longitude	Latitude	Longitude	R_E	Latitude, deg	hours
SCATHA	1200	53.10	274.52	63.52	271.43	6.08	7.45	5.99
	1300	53.28	276.84	63.84	289.34	5.81	9.71	7.18
GOES 7	1200	54.00	270.70	64.14	266.07	6.62	9.71	5.61
	1300	54.57	271.19	64.75	281.38	6.62	9.70	6.60
GOES 6	1200	56.27	240.07	62.34	226.76	6.62	3.74	3.04
	1300	56.62	240.63	62.77	241.99	6.62	4.10	4.03
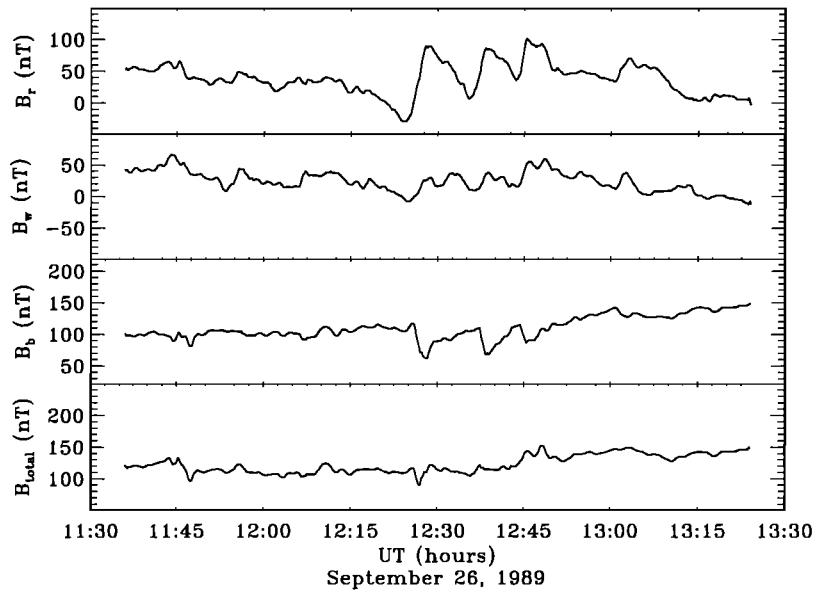
Figure 5. SCATHA observed strong rotations of the field up to 60 degrees, while the field magnitude remained almost unchanged. Data smoothed with 1 min running average.

(when B_r is large) orientations. The r and b components vary systematically with a period of about 10 min. It is significant to note that while SCATHA and GOES 7 are nearly collocated, they witness vastly different field configurations as shown in Figure 6. SCATHA sees large-amplitude rotations $((\Delta B_r/B_r) \approx 1)$ that occur within the tail-like envelope defined by the GOES 7 data. Note that SCATHA is earthward of GOES 7 by only $0.5\,R_E$ and 2° equatorward and south in magnetic latitude, suggesting a fairly localized and time-varying magnetic structure.

DMSP F6 and F8 overflew the region at 1230 UT, with F8 following almost in the track of F6, 2 min behind, both at an altitude near 450 km. The downward precipitating electron and ion fluxes (30 eV - 30 keV) for the two satellites are shown in Plate 1, plotted as a function of latitude. The spacecrafts entered the auroral zone at 56 degrees latitude, and left it at 72 degrees. F6 measured enhanced precipitation from 60 to 63 degrees. Two minutes later, F8 flew through that same region and observed reduced precipitation. This is consistent with eastward drifting patches of electron pre-
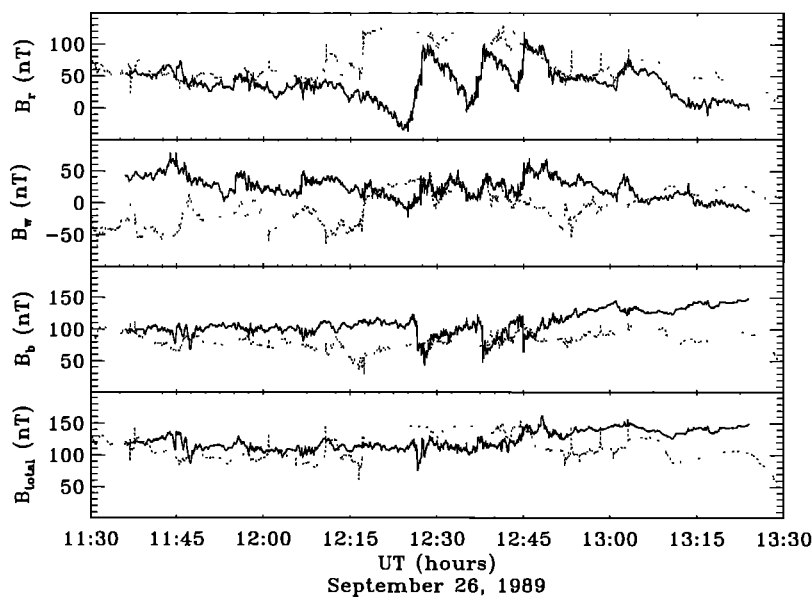
Figure 6. SCATHA and GOES 7 data overplotted. Note that despite the small separation between SCATHA and GOES 7 $(0.5\,R_E)$, they observe vastly different magnetic field signatures.
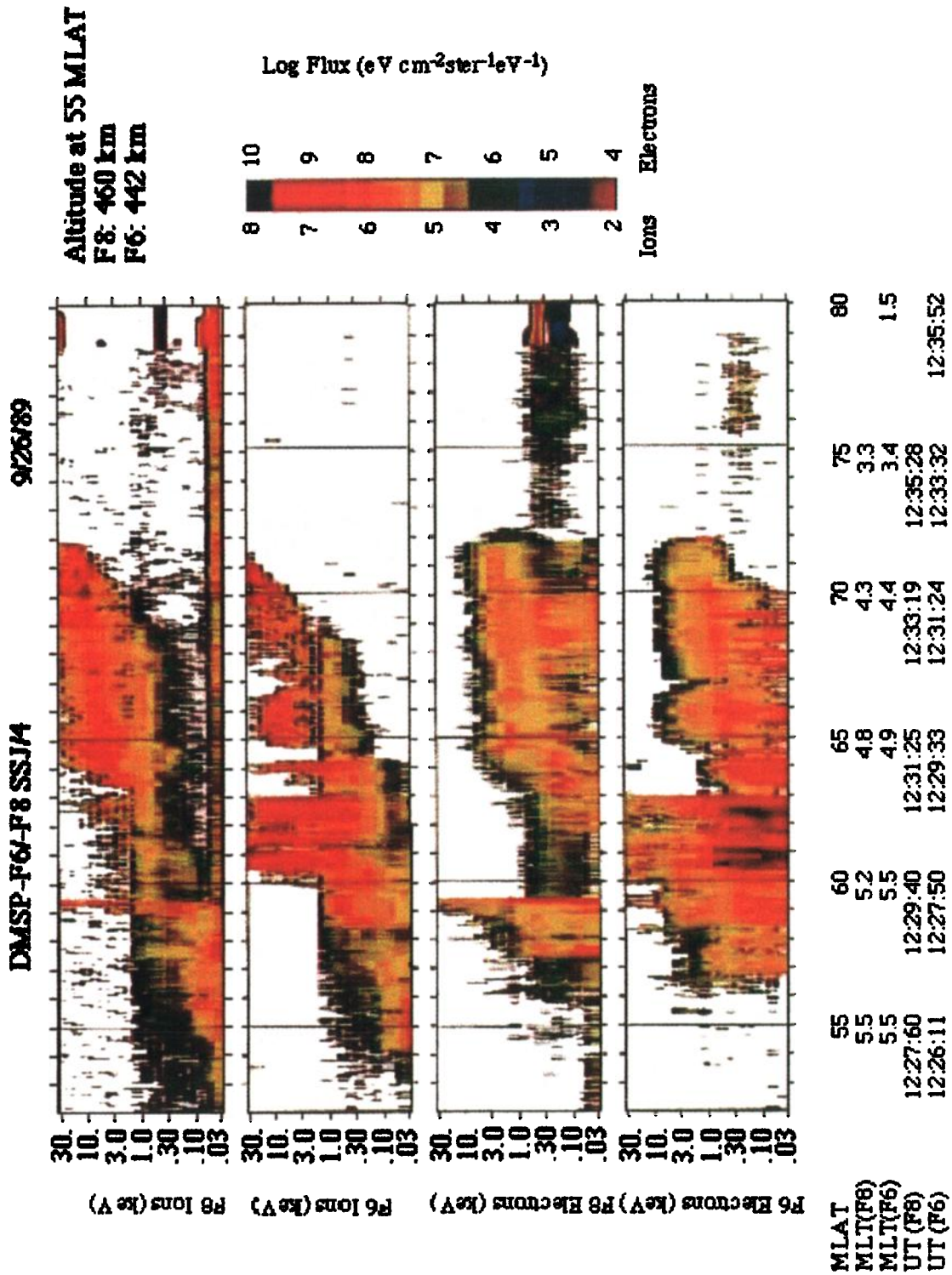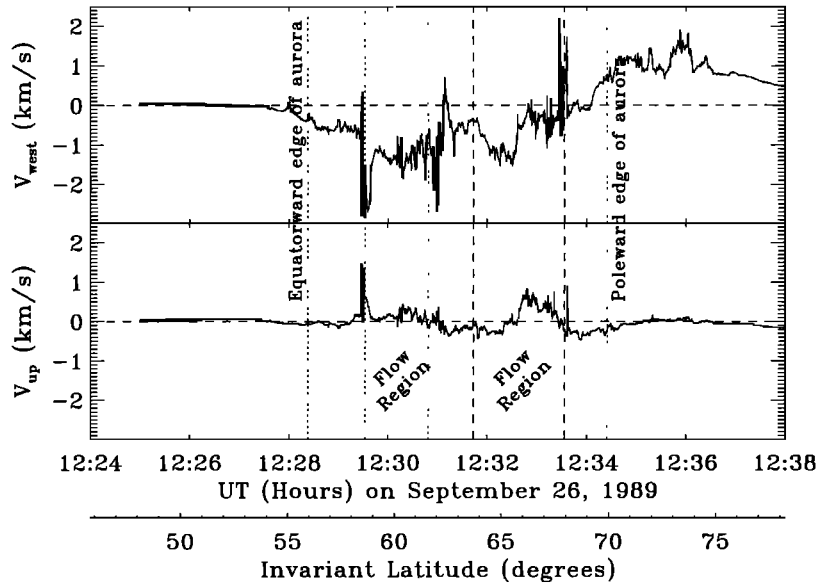
Plate 1. Spectrograms of precipitating electrons and protons for DMSP F6 and F8. Both spacecraft can be seen to enter the electron aurora at 56 degrees and leave it again at 72 degrees latitude. Between 60 and 63 degrees latitude, F6 measured enhanced precipitation, but F8, which passes 2 min later, measures a depletion.

Figure 7. The DMSP F8 drift meter data show two regions of enhanced eastward flow, the more southward one coincident with the region of depleted precipitation. The flow is generally eastward throughout the auroral zone up to the convection reversal boundary just south of the poleward edge of the aurora. The long-dashed lines mark a region that also displays enhanced flows.

cipitation (which are responsible for the bright patches in omega bands); DMSP F6 flew through a bright auroral region stimulated by intense electron precipitation (upward current), the patch drifted eastward for 2 min, then DMSP F8 flew through the "trailing" dark patch (downward current) that shows up as an absence of precipitation.

The F8 ion drift meter measures enhanced eastward flows in the region from 60 to 63 degrees as shown in Figure 7, with especially large eastward flows in the boundary of this region. This is further evidence to support the claim of eastward drifting patches. Also, it should be noted that these features are well south of the poleward edge of the aurora, suggesting that they map to the inner magnetosphere rather than to the low-latitude boundary layer or plasma sheet boundary layer. The regions of enhanced flow have been overplotted in Figure 8 which has the same plot format as Figure 2.

The twin radars Nipawin and Red Lake that make up the BARS field of view are able to measure two-dimensional (2-D) ionospheric plasma flows. We used 30 s resolution data to reproduce what the ionospheric flows would look like if the radars were observing a fixed structure drifting through the field of view of BARS at a constant velocity. The image has been produced in Figure 9 as it would look at 1230 UT, and the CANO-PUS stations and satellite magnetic foot points have been added as well as the field of view of BARS. Note the strong southward flow at 335° longitude which correlates well with the signature at 1230 UT in the GOES 7 B_r and B_w traces. The flow patterns passing the longitude of the GOES 7 foot point earlier, did so further
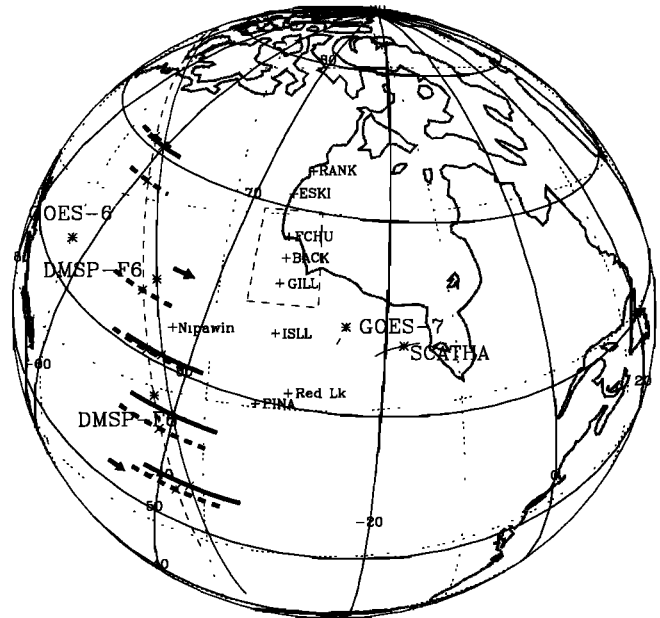
Figure 8. Here we have plotted the flow and precipitation boundaries (identified in Plate 1) encountered by the DMSP satellites onto the same type of projection as used in Figure 2. The solid boundaries are encountered by F6, whereas the dashed ones are encountered by F8. For F6 the boundaries are (from bottom to top): equatorward edge of aurora, equatorward edge of enhanced precipitation, poleward edge of enhanced precipitation, poleward edge of aurora. For F8 the first three boundaries are the same (except that it is a depletion), the next two lines mark the poleward enhanced flow region marked as two dashed lines on Figure 7, and the last boundary is the poleward edge of the aurora.
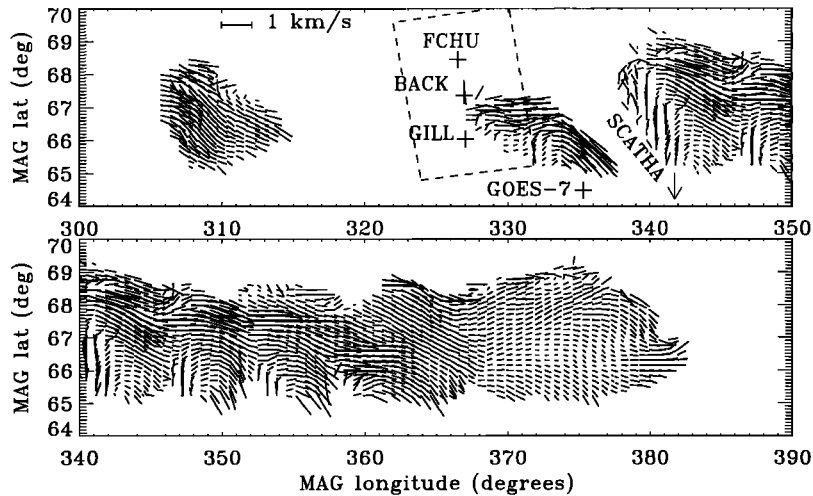
Figure 9. We have produced a snapshot (for 1230 UT) of the ionospheric flows at the latitude of the BARS array from the assumption that the flows measured by BARS are really a fixed structure drifting through the field of view with a velocity of 1.2 km/s. Notice the patches of alternating northward and southeastward flows. Note also the very strong southeastward flow at 335 degrees longitude, which correlates very well with the dips in GOES 7 B_r and B_w (see Figure 4).

north, and were therefore not seen in the geostationary magnetometer data.

3. Discussion

In the preceding section we have presented an impressive array of data from the ground and space from many different types of instruments. In this section we use these data to establish the critical linkage between the

aurora/ionosphere and equatorial magnetosphere that were not tenable in previous studies. In the three panels of Figure 10, we have overplotted the ground magnetometer signatures (scaled and offset) on the spacecraft magnetometer signatures with a time offset, to try to match up features as best as possible. In making such a comparison, we assume that a large-scale 3-D current system flows into, through, and out of the ionosphere and closes somewhere in the magnetosphere. Magne-
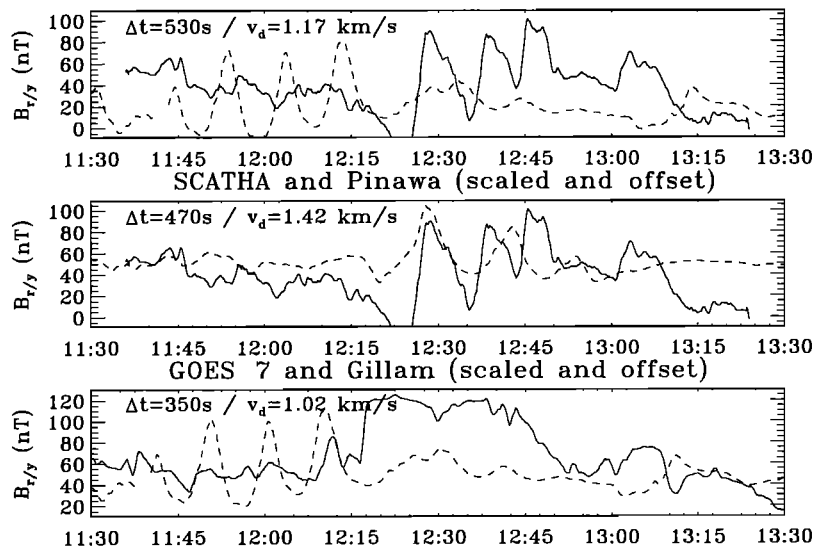

Figure 10. Plot of ground signatures and satellite signatures together. The solid lines are the satellite B_r traces, and the dashed lines are the ground signatures, which have been rescaled, and offset in order to fit on the same graph, and have been shifted in time in order to show the correspondence of pulsations between ground and space. Note that the satellite radial component is compared with the ground east component [*Hughes*, 1983]. These results form the basis for the drift assumed in the generation of Figure 9.

tometer variations reflect this spatially structured an
time-variable current system seen both on the groun
and in space. Because of ionospheric rotation [*Hughes*
1983], one should compare the spacecraft radial ($\hat{r}$) com
ponent to the ground east (Y) component. By matching
up the ground signatures with the spacecraft signature:
with a uniform time shift of the ground time series.
we can calculate an approximate phase velocity of the
waves by measuring the longitudinal offset of the foot
point of the satellite from the location of the magne-
tometers. We calculate velocities of approximately 1.2
km/s. In generating Figure 9 we superposed and av-
eraged BARS images displaced along a constant dipole
latitude by the distance it would have traveled at that
speed since 1230 UT. It should be pointed out here that
the velocity of 8 km/s that the compressional structure
in Figure 4 propagates at is different from the 1.2 km/s
velocity at which the Ω bands are found to propagate.
It appears that the strongest Ω band signatures propa-
gate inside this region, but at a much smaller velocity
than the calculated azimuthal propagation velocity of
8 km/s. It is possible that the 8 km/s velocity is an
artifact owing to the compressional structure not prop-
agating azimuthally, but perhaps nearly radially. This
is an issue that cannot be resolved without more mea-
surements.

The similar appearance of B_x, B_y, and B_z as well as
riometer absorption at Gillam and Pinawa after 1215
UT shows that after that time the two stations are ob-
serving the same set of Ω bands, which thus extend in
latitude to at least cover those two stations. For in-
stance. the riometer dip at 1220 at Pinawa corresponds
to the dip at 1225 at Gillam. Northern stations see
the features later than southern stations at the same
magnetic longitude because of the southeast-northwest
orientation of the current system. The 1220-1225 cur-
rent system thus passes over both stations. Subsequent
current systems pass further south over Pinawa, as wit-
nessed by weaker magnetometer and, almost absent, ri-
ometer signatures at Gillam.

It is possible that the trains of pulsations seen at
Gillam before 1210 and at Pinawa after 1215 UT are ei-
ther two different trains of pulsations, or that the cen-
ter of the pulsations shifted south between 1210 and
1215. The intense southeastward flow, deduced from
the BARS data to exist at 335° magnetic longitude
(Figure 9) at 1230, corresponds to the dip in B_r and B_w
seen at GOES 7 (Figure 4) at 1230. This current system
was also observed at Gillam at 1225. The BARS data
show that this current system was further south than
the train that passed Gillam between 1140 and 1210. It
thus passed at the latitude of GOES 7, and stretched to
the latitude of SCATHA, where it was observed as the
first in a series of three peaks. The following peaks were
observed only weakly at GOES 7 due to their being too
far equatorward and were not observed in the BARS
data. This suggests that the Ω band source regions in
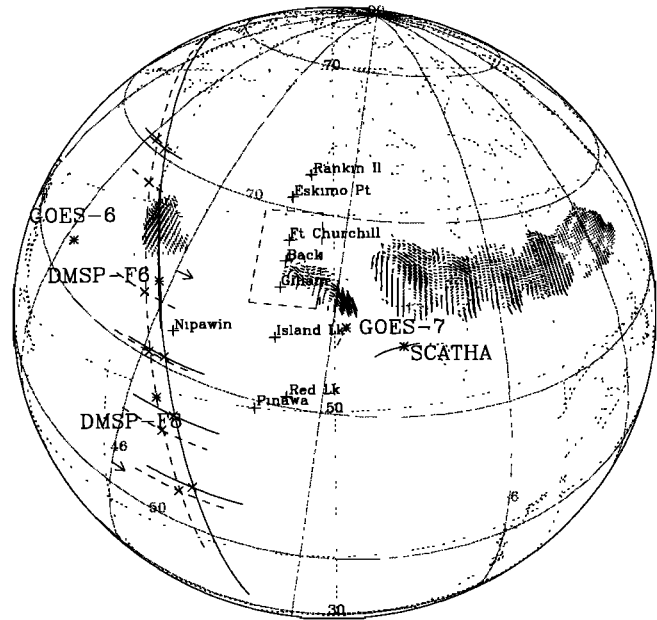
Figure 11. Similar to Figure 8, but has the BARS
flow data added to it. It clearly shows the northern
wave train passing through BARS and over Gillam. In
the southeastern corner of the BARS field of view can
be seen the flow which is associated with the rotation
of the GOES 7 magnetic field at 1230 UT.

the equatorial magnetosphere are very localized. The
passage on the ground of each Y peak corresponds to
the passage of a bright auroral spot (as shown by the dip
in the riometer trace), and the upward current branch in
the 3-D current system. The downward current branch
occurs in the dark spots in between, and the passage of
such a set of up-down currents (which appear as an in-
verted Ω in auroral images) appears as a Ps6 pulsation.

The two eastward flow regions marked on Figure 8
can be interpreted as the latitude ranges in which the
two trains of omega bands flow. The first train passes
in the northernmost channel, then another train passes
in the southernmost channel. It can be seen from Fig-
ure 8 that SCATHA does not appear to map within
the southern flow region as measured by DMSP F6 and
F8. There are three different interpretations: either
(1) the omega bands are not actually confined within
this flow region; (2) the flow region moved northward
between the longitude of DMSP and the longitude of
SCATHA; or (3) the magnetic field model used (T89
with $K_P = 5+$) is not capable of describing the field,
and thus not capable of accurately mapping the space-
crafts to the ground. We favor the latter, since exami-
nation of the magnetic field on SCATHA and GOES 7
suggests a field geometry much more stretched than the
model is capable of describing. A more stretched field
would result in mapping the satellite foot points to a
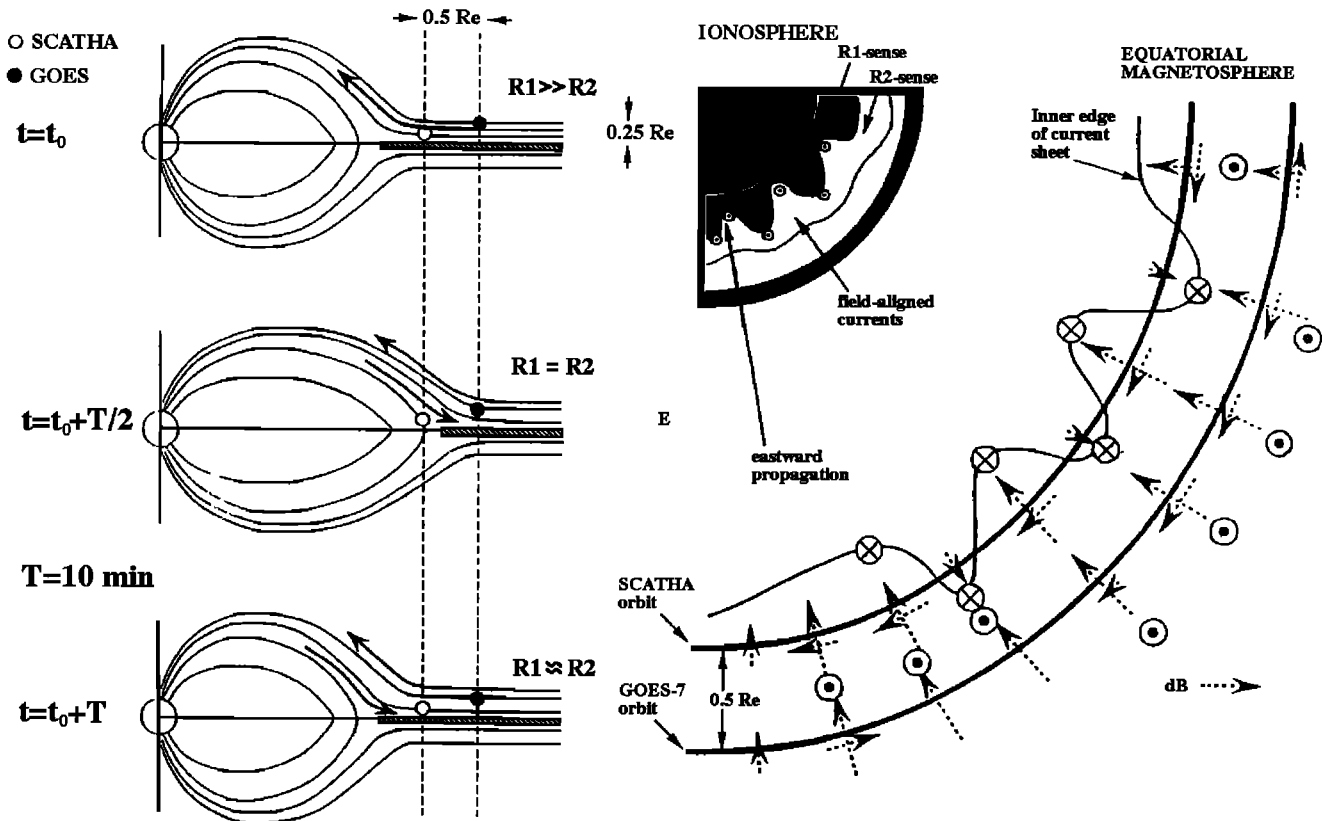lower latitude.

Figure 12. Magnetospheric as well as ionospheric perspectives on a possible scenario.

Figure 11 is similar to Figure 8, but has the BARS flow data added. It clearly shows the northernmost wave train passing through BARS and over Gillam, and the beginnings of the more southern wave train, which passes over SCATHA/Pinawa, and close to GOES 7. The DMSP spacecrafts observe the flow region in which these wave trains propagate in the ionosphere, as well as some indication of alternating dark and bright patches supporting the riometer observations.

4. Conclusion

Omega bands map in this case to near (both inside and outside) geostationary in the equatorial plane. This agrees somewhat with the T89 model for maximum stretching, even though it is evident that the field at the location of SCATHA and especially GOES 7 is even more stretched than the model can produce (a positive B_r indicates a stretching when we are above the magnetic equator). Also, at the location of SCATHA, the field appears to vary between dipolar, and very stretched with a period of 10 min, suggesting a highly distorted and dynamic field geometry adjacent to a quiet and stretched field. The mapped positions of GOES 7 and SCATHA suggest that the field shows signs of a tail-like (or highly stretched) geometry at 6 MLT. Such configurations have been observed before

but only routinely discussed in the context of severe growth phase stretching just prior to onset near 00 MLT [*Fennell et al.*, 1996].

We suggest that omega bands map to near geostationary orbit into a source location where large-scale MHD waves propagate in some yet to be determined boundary. The boundary could be interpreted as the sharp inner edge of a very intense disk current at the equator, although this conclusion is not necessarily unique. The waves produce large-amplitude field rotations, which in turn are equivalent to large induced electric fields. The induced electric fields (which are field aligned for pure rotations) could be sufficient to cause acceleration of electrons that then precipitate to cause the bright auroral spots that are observed on auroral images, as well as contribute to one leg of the current loop responsible for Ps6 pulsations.

A possible scenario for this coupling is sketched in Figure 12. An oscillation at the inner edge of the plasma sheet produces a corrugated current structure. This interface is drawn so as to separate the large-scale Region 1 / Region 2 FACs, which is consistent with our observations. The FACs near this current meander produces the observed variations on the ground as well as near the equatorial plane.

While Figure 12 is one possible interpretation and appears to be well constrained by the data, it is not

yet clear if other current patterns could produce similar signatures. Our results definitively place the source region of Ω bands close to the Earth. *Pulkkinen et al.* [1991] has suggested a similar source region, but based only on simple empirical magnetic field mappings. As such, present theories that have described Ω band wave generation in the magnetosphere will now have to be reinvestigated in light of a very different particle and field regime than traditionally considered. These aspects of this interesting new set of observations are the focus of a future study.

References

Akasofu, S.-I., E. W. H. Jr, M. D. Montgomery, S. J. Bame, and S. S. Singer, Association of magnetotail phenomena with visible auroral features, *J. Geophys. Res.*, *76*, 5985–6003, 1971.

Connors, M., and G. Rostoker, Source mechanisms for morning auroral features, *Geophys. Res. Lett.*, *20*, 1535–1538, 1993.

Fennell, J., J. Roeder, H. Spence, H. Singer, A. Korth, M. Grande, and A. Vampola, CRRES observations of particle flux dropout events, *Adv. Space Res.*, *18*, (8)217–(8)228, 1996.

Hughes, W. J., Hydromagnetic waves in the magnetosphere, in *Solar-Terrestrial Physics*, edited by R. L. Carovillano and J. M. Forbes, pp. 453–477, D. Reidel, Norwell, Massachusetts, 1983.

Kawasaki, K., and G. Rostoker, Perturbation magnetic fields and current systems associated with eastward drifting auroral structures, *J. Geophys. Res.*, *84*, 1464–1480, 1979.

Peredo, M., N. A. Tsyganenko, D. P. Stern, and T. Sotirelis, Geopack: An improved library of data-based models of the magnetospheric magnetic field, Paper GAB51H-02 at the IUGG XXI General Assembly, Boulder, Colorado, July 2-14, 1995.

Pulkkinen, T. I., R. J. Pellinen, H. E. J. Koskinen, H. J. Opgenoorth, J. S. Murphree, V. Petrov, A. Zaitzev, and E. Friss-Christensen, Auroral signatures of substorm recovery phase: A case study, in *Magnetospheric Substorms*, Geophys. Monogr. Ser., vol. 64, edited by J. R. Kan, T. A. Potemra, S. Kokubun, and T. Iijima, pp. 333-341, AGU, Washington, D.C., 1991.

Rostoker, G., and J. C. Barichello, Seasonal and diurnal variation of ps6 magnetic disturbances, *J. Geophys. Res.*, *85*, 161–163, 1980.

Rostoker, G., and J. C. Samson, Can substorm expansive phase effects and low frequency Pc magnetic pulsations be attributed to the same source mechanism?, *Geophys. Res. Lett.*, *11*, 271–274, 1984.

Tsyganenko, N. A., Global quantitative models of the geomagnetic field in the cislunar magnetosphere for different disturbance levels, *Planet. Space Sci.*, *35*, 1347, 1987.

Tsyganenko, N. A., Magnetospheric magnetic field model with a warped tail current sheet, *Planet. Space Sci.*, *37*, 5–20, 1989.

A. M. Jorgensen, Los Alamos National Laboratory, Space and Atmospheric Sciences (NIS-1), MS D466, Los Alamos, NM 87545.

H. E. Spence, Center for Space Physics, Boston University, 725 Commonwealth Ave., Boston, MA 02215.

T. J. Hughes and D. McDiarmid, Herzberg Institute of Astrophysics, National Research Council, Ottawa, Ontario, Canada K1A 0R6.